Glacier snow sub-surface properties on Svalbard in the atmospheric model WRF

SVALI DELIVERABLE D3.1-5/D2.3-2

Report

BJÖRN CLAREMAR

SVALI POSTDOC

DEPARTMENT OF EARTH SCIENCES

UPPSALA UNIVERSITY

NOVEMBER 2014–JANUARY 2015

UPPSALA UNIVERSITET

ABSTRACT

Snow accumulation is a complex process and difficult to model due to the uncertainties in precipitation but also in the melting and what happens with the melt water in the snow pack. Additionally the redistribution of the surface snow can be significant in exposed areas. This report investigates the process of the retention and refreezing of melt water on Svalbard and the sensitivity of a number of parameters in the atmospheric model WRF. It continues the work in the SVALI report 3.1-1 by analysis of output from the 5-layer snow scheme in CLM4 land surface model in addition to the 3-layer Noah-MP. The performance of the two snow schemes is investigated in relation to snow observation at Lomonosovfonna, which were not available for the earlier report. The investigated parameters include water holding capacity in the pore space in the snow, heat conductivity of the snow, the maximum snow water equivalent w.e. handled by the snow scheme and initialization of the snow/firn/glacier temperature.

The simulations and the analysis gave rise to some new questions and could not directly answer the ones asked. It could for instance not be determined which of snow thermal conductivities and water holding capacity is the better one. The analysis suggests that the snow thermal conductivity is much more important than the water holding capacity (in the range 1–3%) in determining the melt and snow temperature evolution. It was however shown that the initialisation of the snow properties is very important. The best seems to be setting the deep layer temperatures layers to 0°C and allow for at least one year of spin-up. CLM4 is more sophisticated but very computationally expensive. Therefore Noah-MP must be used for climate simulations (at least if run in Uppsala). The belief is that by including the firn layers below the snow layers in the model above the ELA, three snow layers may be sufficient. However, ice lenses will not be possible to simulate, except in the uppermost layers of the snow. Further work, trying to answer the new questions and by utilizing observation from more sources, will be performed in a coming manuscript (D3.1-2).

INTRODUCTION

Surface mass balance for snow (SMB) is a complex process and difficult to model. Firstly the modelled precipitation is associated to large errors (this is one of the most difficult meteorological variables to simulate). Then also the partition of snow and rain is also important (and rather uncertain). At the snow surface the wind can also redistribute the snow but with sufficiently large area averages this is of minor importance. Further, the surface sublimation and snow melt must be determined. However, the melting snow or rain will percolate in the snow pack and will partly be retained in the pores by capillary forces or refreeze on its way down, depending on the cold content in the snow. This means that melting will not necessarily give negative surface mass balance in the summer. With rain water refreezing in the snow the SMB can even be positive. If the melt water in the snow on a glacier percolates down to the firn, the observed annual mass balance will not be correct and we have an internal accumulation, i.e. accumulation not measureable in the annual snow. The formation of ice lenses and preferential flow or "flow fingers" also complicates the way to model the way down of melt water in the snow pack. It is interesting to model the SMB directly from the atmospheric model but the most important issue for the atmospheric model itself is to find the onset of glacier or ground exposure to the air when the snow is gone, since this effectively changes the surface–air interaction in terms of surface turbulence fluxes and radiation balance.

At the water retention workshop at DTU, Copenhagen in October 2014 the following bullet points, describing the needs of research, were established:

- Better estimates/understanding of the processes that control melt water transitions from percolation in firn to preferential flow in firn to horizontal routing of water that eventually become supraglacial streams.
- In the percolation area we can estimate melt water retention because by definition it does not exit the cold snow. And, in zones with no or very limited firn overlaying solid ice algorithms are available for quantifying the development of superimposed-ice. Yet, we need to improve retention understanding/quantification in the remaining areas and come up with common rules/algorithms.
- For better process understanding a combination of physical and stochastic modelling should be established.
- Observation on temporal and spatial evolution is key to understanding governing physical processes.

This report continues the work presented in the SVALI report D3.1-1 (Claremar 2013b). It investigates the sensitivity in changing some of the physical parameters in the snow schemes, both in the CLM4 and in Noah-MP land surface schemes of the atmospheric model WRF (Noah-MP was used in the earlier report). These parameters include water holding capacity in the pore space in the snow, heat conductivity of the snow and snow depth taken into account in the model. Hence this study is mostly related to bullet 3 and the stochastic modelling or rather statistical, in the way that we rather tune the parameters to resemble the average of temperature measurements. Over Svalbard the glaciers are either in the ablation zone, where we have no internal accumulation (but superimposed ice may form on the hard glacier

surface), in the cold zone (at least earlier above 900–1200 m in NE Spitsbergen and above 550 m on Vestfonna and Austfonna (e.g. Shumskii 1955, 1964, Dunse et al. 2009)) or in the warm percolation zone, where we have the least knowledge in quantifying the water retention according to bullet 2.

The choice of CLM4 in addition to Noah-MP was motivated by the more sophisticated albedo scheme and more snow layers (5 compared to 3). However it was found that it is more CPU-demanding and not suited for climate simulations on the computer cluster used by the author. Comparison between model simulations and observations from Lomonosovfonna (in the warm percolation/infiltration zone) are performed (Marchenko 2013).

The research questions are how the two snow schemes perform relative to the snow observations and if optimal expressions of snow thermal conductivity and water holding capacity can be found? Further, can we without too much problems use the more effective (in time) Noah-MP model for climate simulations?

MODEL AND MEASUREMENTS

WRF Model

The WRF model (Skamarock et al. 2008) is an open source model (http://www.mmm.ucar.edu/wrf/users/) widely used in research and is useful in ranges 100 of kilometres down to finer than 1 km horizontal resolution. The model output used in this investigation had horizontal resolution of 16.5 km and the model set-up was basically that of the study by Claremar et al. (2012) but for the WRF3.6 version (not polar WRF). In Claremar et al. (2012) various physics schemes were changed in a sensitivity study. Here we use the Morrison double-moment microphysics scheme (Morrison et al. 2005) and the MYNN2.5 turbulence schemes (Nakanishi and Niino 2006) and the CLM4 land surface scheme (Niu et al. 2011). Forcing data were from the ERA-Interim re-analysis (Dee et al. 2011). The sea surface temperature (SST) is taken from OSTIA (Donlon et al. 2012) where the resolution is as fine as 0.05° (i.e. 5.5 km in N-S direction and about 1 km in W-E). Terrain and land use data are originally from USGS (U.S. Geological Survey) but here the land use/glacier mask is taken from NPI (Nuth et al. 2013). Fig. 1 shows the model grid and terrain and the glacier investigated.

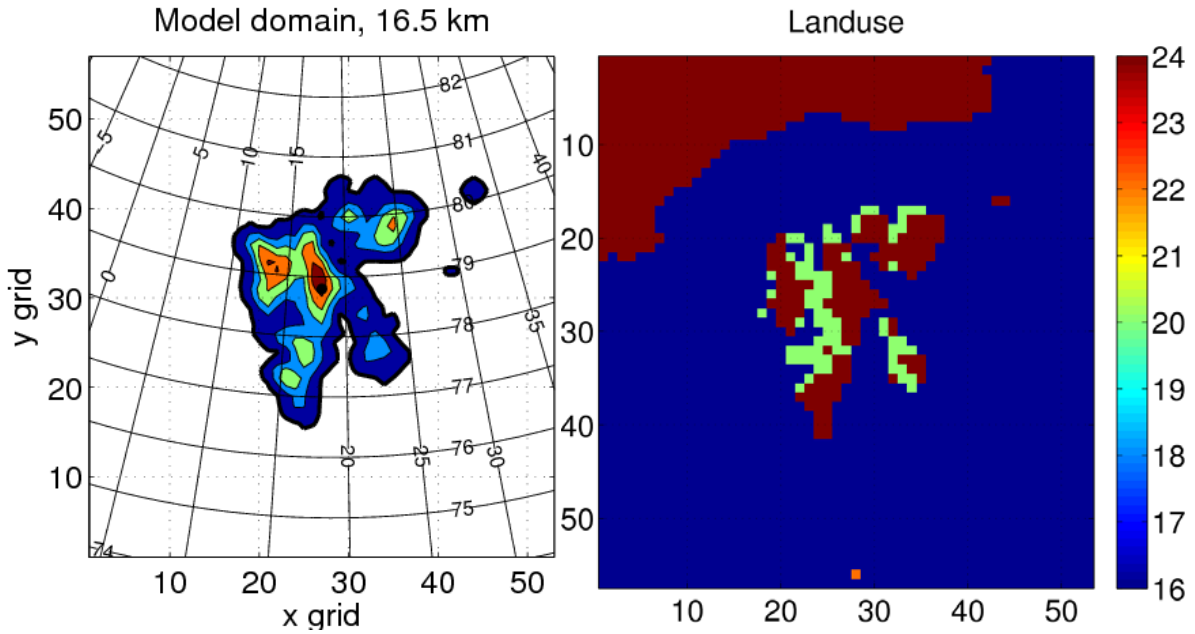

Figure 1. In a) model domain and Lomonosovfonna marked by dot. Contour lines show elevation with 200 m equidistance. In b) NPI landuse with dark red being glacier or sea ice, green tundra and blue water.

Snow scheme

In the WRF model several different land surface models/schemes (LSMs) can be used. In a previous report (Claremar 2013b) the Noah-MP scheme (Niu et al. 2011, Yang and Niu 2003) was used. It has 3 snow layers and liquid water retention and refreezing already implemented. Snow compaction is accounted for, following Anderson (1976) and Sun et al. (1999). It was found in the report that 3 layers gave too coarse resolution in the thermal and hydrological development in the snow. Depending on the snow depth the snow consists of one to three layers. Uppermost layer is limited to 5 cm, the middle one to 20 cm (adding up to 25 cm) and the lowest is limited by the snow depth which in turn is limited by maximum 2 m water equivalents (mwe) and thus can be several meters thick, depending on the density. This thick layer limits the possibility to describe the snow evolution and work with the introduction of more layers was started but cancelled. The architecture of the program code delimited the possibility to do so in the available time frame. However, the soil layers in the Noah-MP scheme uses firn/glacier properties. The firn layer thicknesses are constant, being 0.1, 0.3, 0.6 and 1 m, counting from above and adds up to 2 m. Densities are not explicitly calculated but thermal conductivity and capacity are functions of depth. Liquid water and refreezing is accounted for and can be tracked but the water holding capacity is unlimited. Albedo is from the BATS scheme (Yang et al., 1997). Division of snowfall and rain is done following the relatively complex functional form of Jordan (1991).

In the present study this scheme is used as well and in addition simulations with CLM4 scheme are performed (Lawrence et al. 2011). It has up to 5 snow layers and more sophisticated albedo scheme (SNICAR). The layer thicknesses for deep snow are, counting from surface, 2, 5, 11, 23 cm (41 cm) and for the deepest layer about 100 cm, depending on

the density and w.e. (maximum 1 m). The performance of the albedo scheme and possible updates will be investigated in coming work. In the present study we focus on the snow hydrology.

Thermal conductivity

The thermal conductivity of the snow, k_{snow}, is needed to calculate the time evolution of the snow temperature:

$$C_{snow}\frac{\partial T_{sno}}{\partial t}=\frac{\partial}{\partial z}\left(k_{snow}\frac{\partial T_{sno}}{\partial z}\right)+S$$

where the volumetric heat capacity is given by

$$C_{snow}=C_{ice}\theta_{ice}+C_{liq}\theta_{liq}$$

where θ_{ice} and θ_{liq} stand for partial volume of ice and liquid water and C_{ice} and C_{liq} are the specific heat capacity of water and ice at constant volume ($4.188\cdot10^6$ and $2.094\cdot10^6$ J/m^3/K), respectively. S is a source/sink term including surface heating and phase changes. Volumetric heat capacity for the firn in Noah-MP is given by the "Noah glacial ice approximation":

$$C_{firn}=\left(0.8194+0.1309D\right)\cdot10^6$$

where D is the mid-layer depth in meters, counted from the firn–snow boundary. This gives values in the range 0.8–1.0 J/m^3/K.

The snow conductivity, k_{snow}, is parameterized as function of bulk snow density, ρ_{snow}, for each snow layer. The original expression in each LSM for the snow conductivity are compared to a third one. The original one in Noah-MP is from Yen (1965):

$$k=3.2217\cdot10^{-6}\rho^2$$

and from Jordan (1991) in CLM4:

$$k=0.023+(7.75\cdot10^{-5}\rho+1.105\cdot10^{-6}\rho^2)\cdot(2.29-0.023)$$

The above original expressions are changed to an expression from Sturm et al. (1997):

$$k=0.138-1.01\cdot10^{-3}\rho+3.23\cdot10^{-6}\rho^2$$

The difference between all expressions is shown in Fig. 2. For low densities (new snow) the original expressions are very similar but for ρ higher than 200 kg m^{-1} Sturm et al. (1997) gives lower values. The Sturm et al. (1997) and Jordan (1991) converge for zero density at 0.023 W K^{-1} m^{-1}, which is the thermal conductivity for air. In Jordan (1991) the thermal conductivity reaches 2.2 W K^{-1} m^{-1} for pure ice at 917 kg m^{-3}. We choose the expression from Sturm et al. (1997) before other studies because this paper presents a very thorough investigation of many studies and points out earlier shortcomings. In Fig 2, one can also see

that the Yen (1965) study was based on a limited range of densities. The firn thermal conductivity is given by "Noah glacial ice approximation":

$$k_{firn} = 0.32333 + 0.10073D\,,$$

where D is the mid-layer depth in meters, counted from the firn–snow boundary. This corresponds to k_{firn} in the range 0.33–0.47 W K^{-1} m^{-1}, i.e. density ranges of 300–400 or 450–500 kg m^{-3}, using Jordan (1991) or Sturm et al (1997) expressions, respectively (see Fig. 2). These densities are rather low, especially if the Jordan (1997)/Yen (1965) expressions are more valid. Shown in Fig 2 is also an expression by Domine et al. (2011). Since we are interested in a sensitivity analysis we omit simulations with this expression since it is in between the above mentioned expressions.

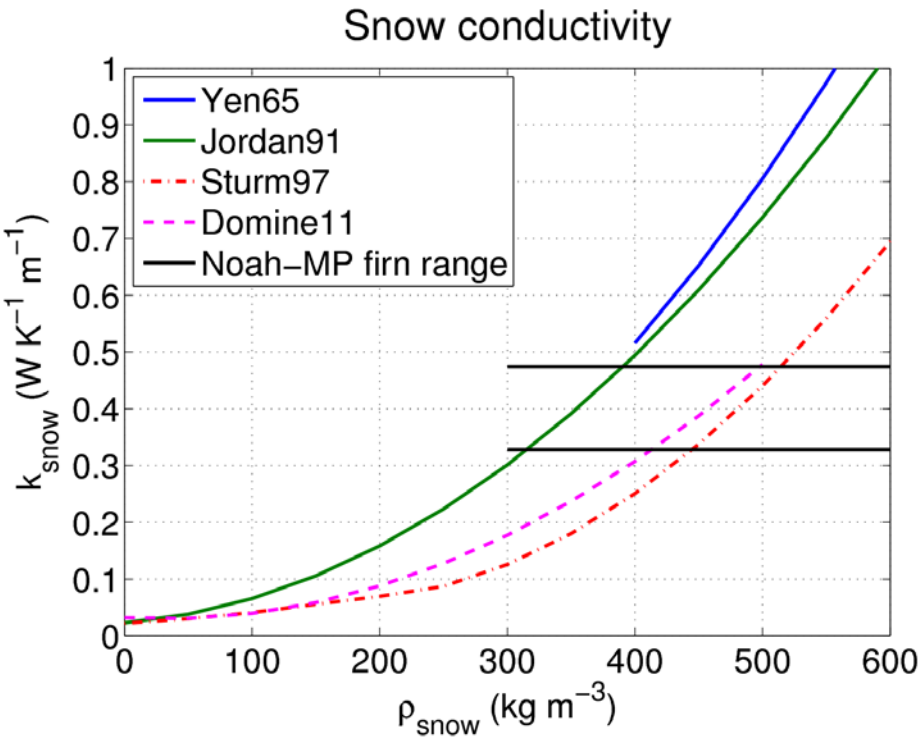

Figure 2. Thermal conductivity in the snow.

Liquid water in snow pack

Liquid water description in the snow is already implemented in Noah-MP and CLM4 and dependent on melting, rainfall, the available pore space and the water holding capacity, WHC, or in other words irreducible snow water saturation, SSI, of the snow pack. The water that does not freeze because of too small amount of cold content in snow layer and is not held by the water holding capacity percolates down to the next layer but can also be prevented from this if the lower layer already is saturated.

The flow from one layer *i* is given by:

$$0 \le q_{out,i} = \left(\theta_{liq,i} - \mathrm{SSI} \cdot \theta_{pore,i}\right) dz_i < \theta_{pore,i} - \theta_{liq,i}$$

If the pore space is less than 5% in a layer (ρ_{snow}>850 kgm^{-3}) it is considered impermeable. Therefore the percolation is set zero if the actual layer OR the layer below has a pore space below 5 %. The lowest snow layer has a free drainage. The original code has a constant SSI=0.03 in Noah-MP and 0.03 in CLM4. We also test SSI=0.02 (WHC2) which may account for preferential flow that increases the percolation.

Snow initialisation

It is of importance that the snow temperature profile is well reproduced during the winter before the analysis period since this will affect the amount of melting, retention and refreezing in the snow later on. This is because of the cold content of the snow. Therefore the model has to spin up. It was first decided to start the initialization of the model at the start of the hydrological year, 31 Aug 2011. It was also tested to start the simulations one year before, in 1 Sep 2010. The depth of snow taken into account in the model will also affect the evolution of the snow temperature. How will the deep snow temperature affect the winter cold? This requires sufficiently deep snow in the calculations, but will be limited by the large thickness of the deepest snow scheme layer. The limiting snow depth is dependent on the density because the snow w.e. is limited in the model. In some sensitivity tests the Noah-MP limit was increased from 2 m to 5 m w.e. and in CLM4 it was increased from 1 to 5 m w.e. This corresponds, in the simulations presented here, to 10 m for Noah-MP. In CLM4 this limit was never reached because the initial snow is reduced to almost zero but during two years at Lomonosovfonna 3 m of snow was reached.

Analyses of the mentioned simulations prompted tests with other temperature profiles already at the spin-up start. Firn temperature and also deep climatologic temperatures (basically a boundary condition to the deepest firn layer) was set to 0°C as well.

MEASUREMENTS

We use measurements from two sites which are close to each-other but on different altitudes.

AWS station

For validation of the 2-m temperature simulated by the model we use measurements from an AWS at Nordenskiöldbreen (78°41'39"N, 17°09'22"E, 530 m a.s.l.). The location is shown in Fig. 3. Nordenskiöldbreen is one of the major outlet glaciers of the ca 600 km^2 large Lomonosovfonna ice field draining towards the Billefjorden in the inner part of Isfjorden. The glacier is about 5 km in width and 17 km long. The AWS is situated in the central flow line of the glacier, which is confined by steep slopes to the north and to the south. The direction of the downward slope of the glacier at the AWS site is to southwest. For further details see description of the site in Claremar et al. (2012).

Snow temperature measurements

Observed snow temperatures are taken from nine 10 m long thermistor strings from a location at 1200 m a.s.l. on Lomonosovfonna (Fig. 3). They were put in drill holes separated by 3 m and in a square with the sides 6 m. Thus the local heterogeneity of the temperature was captured. The temperatures were not significantly different between the strings. Ice layers (not analysed here) were, however, highly heterogeneous. The thermistors were installed in mid-April and are placed most often with a vertical distance of 1 m apart. In some strings the distance can be less (around 0.5) close to the surface. An average temperature for each present depth is used for the comparison to the WRF output. Also density and stratigraphy profiles were taken the 13 April. For more details of this site see reports by Marchenko (2012, 2013).

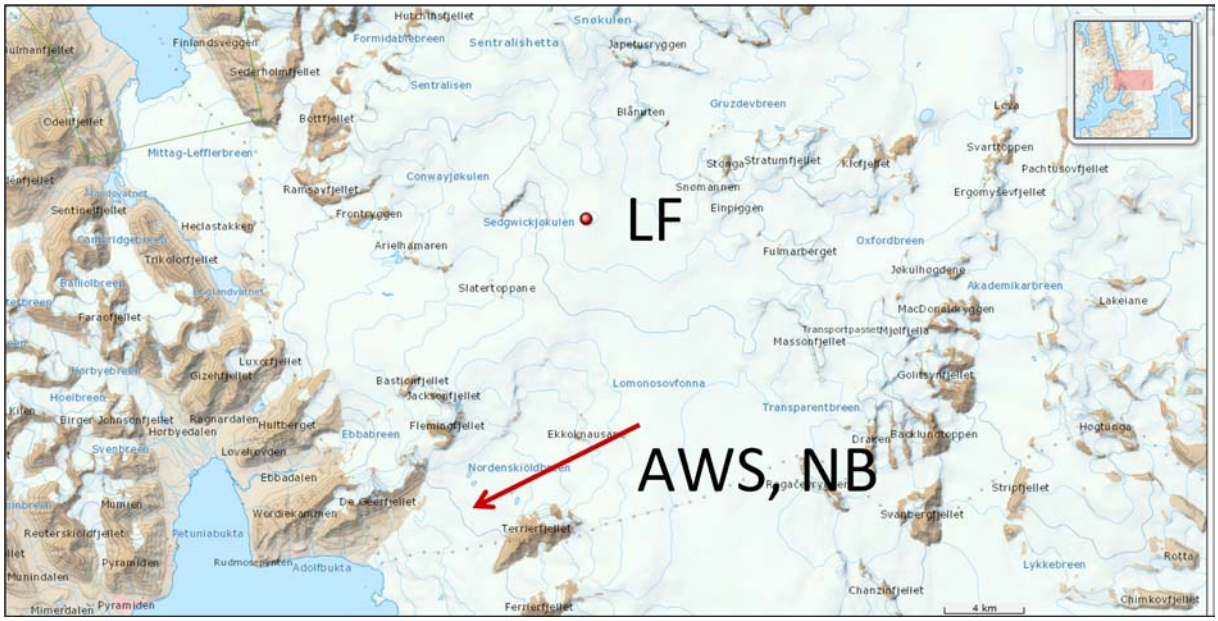

Figure 3. Map of the Lomonosvfonna and Nordenskiöldbreen

METHODOLOGY

The WRF model will produce biases to the observed in air temperature and radiation, among other parameters. To solve for the temperature bias part we use temperature measurements from Nordensköldbreen to find temperatures as correct as possible. This is done by finding the bias in the winter (Sep to June) temperature (to force the onset of the melt period) and surface temperature lapse rate produced in the same period in the model (varying between 5.5 and 5.9°/km in the different simulations). Since there is a cold bias we can find the correct temperature about 300 m further down (corresponding to about 1.8°C). Assuming that the simulated lapse rates are correct, a point was chosen with height 910 m close to Lomonosovfonna (1200 m a.s.l.) and along the north-south ridge (to minimize west/east barrier effects on precipitation).

The different runs performed in this study are summarized in Table 1. Initially the focus was on the CLM4 scheme, but during the progress of the work its focus was transferred to Noah-MP. Note the differences in CPU-time between the Noah-MP and CLM4 simulations. In general the Noah-MP scheme makes the simulations run about five times faster. Further the runs with CLM4 is numerically more unstable. Therefore the changes in the two schemes have not been identical but have mirrored how the interest has changed from the view of the evolving results and CPU-time consumed. The initialization is either on 31 August 2011 or in 2010, to reflect the importance of spin-up for the snow pack. The longer runs are given the index "*2y*". The original physics simulations are given the index "*Ref*", changing the snow heat conductivity to that of Sturm et al. (1997) is called *"Sturm"* and changing the water holding capacity to 2% is indexed by "2". The change of the limiting snow depth in terms of w.e. is given the index "*5 m*".

Comparison of the snow temperature evolution by WRF to the mean of the 9 thermistor strings at *LF* at 1200 m in the summer 2012 is performed. Also the sensitivity to summer melting is shown. In a coming study this will be compared to measured ablation at several glaciers on Svalbard.

Table 1. The simulations performed.

Run	**Comments**	**Approximate CPU-time (hours** x **cores)**
CLM4		
Ref	Original CLM4 snow part of the surface physics scheme	46x32=1500
Ref_2y_5m	Original CLM4 scheme but with more spin-up and 5 m of maximum w.e.	47x48=2300
Noah-MP		
Ref	Original Noah-MP scheme	4x48=200
Ref_2y	As above but with 20 month spin-up	8x48=380
Ref_2y_5m	As above but with maximum of 5 m w.e.	__"__
Ref_2y_1m	As above but with maximum of 1 m w.e.	__"__
Ref_2y_1m_init0	As above but initialisation with 0°C	__"__

	firn	
Ref_2y_1m_glac0	As above but with 0°Cglacier ice and firn	—"—
Ref_2y_2m_glac0	As above but with 2 m w.e. snow	—"—
Ref_2_2y_2m_glac0	As above but with 2% WHC	—"—
Sturm_2y_1m_glac0	As above but with Sturm heat conductivity, 1 m w.e. snow and 3% WHC	—"—
Sturm_2_2y_1m_glac0	As above but with 2% WHC	—"—
Sturm_1_2y_1m_glac0	As above but with 1% WHC	—"—

RESULTS

The analysis focuses on the snow temperature evolution in WRF model in comparison to the measurements at Lomonosovfonna. In Fig. 4 the observed temperature evolution is shown. Since there is snow falling as well as there is melting at the surface snow the snow depth of the thermistors are correct only for the late April when thermistor strings were installed. They are buried during the course of time but it is not known how much. The accumulated snow simulated by WRF and presented in Fig. 5 can be interpreted as the upper limit of the underestimation of the sensors depths. The low daily variation of temperature close to the surface in Fig. 4 suggests that zero depth actually corresponds to at least 10 cm of snow above the upper thermistor during the summer. Therefore we should not look at the surface details in the simulations. The observed deeper snow temperature in Fig. 4 shows a distinct cold wave in May represented by a minimum below –10°C less than 2 m from the surface. Then the heating from above continuously increases the temperature near the surface by thermal conduction, while the depth of the minimum temperature deepens at the same time as the minimum temperature increases. This continues until July/August when a number of events give abrupt increases of temperature and eventually it reaches 0°C in the entire profile. These events are probably due to melt water percolation and refreezing that is accompanied by release of the latent heat. In September the whole snow pack shown in the figure shows close to zero temperatures (–0.2 to 0°C). At that time the upper layers begin to be cooled due to the decreasing air temperature and downwelling short-wave radiation. In the end of August there is also a cold spell that is seen in a drop of the temperature within a meter of the snow pack. It can also be noted that the cold wave reaches 12 m. It can also be noted that the very deep layers seems to be heated from below. In the comparison with the simulations just the upper 4 to 10 meters of the observed snow temperature will be valuable, depending on the thickness of the snow model domain.

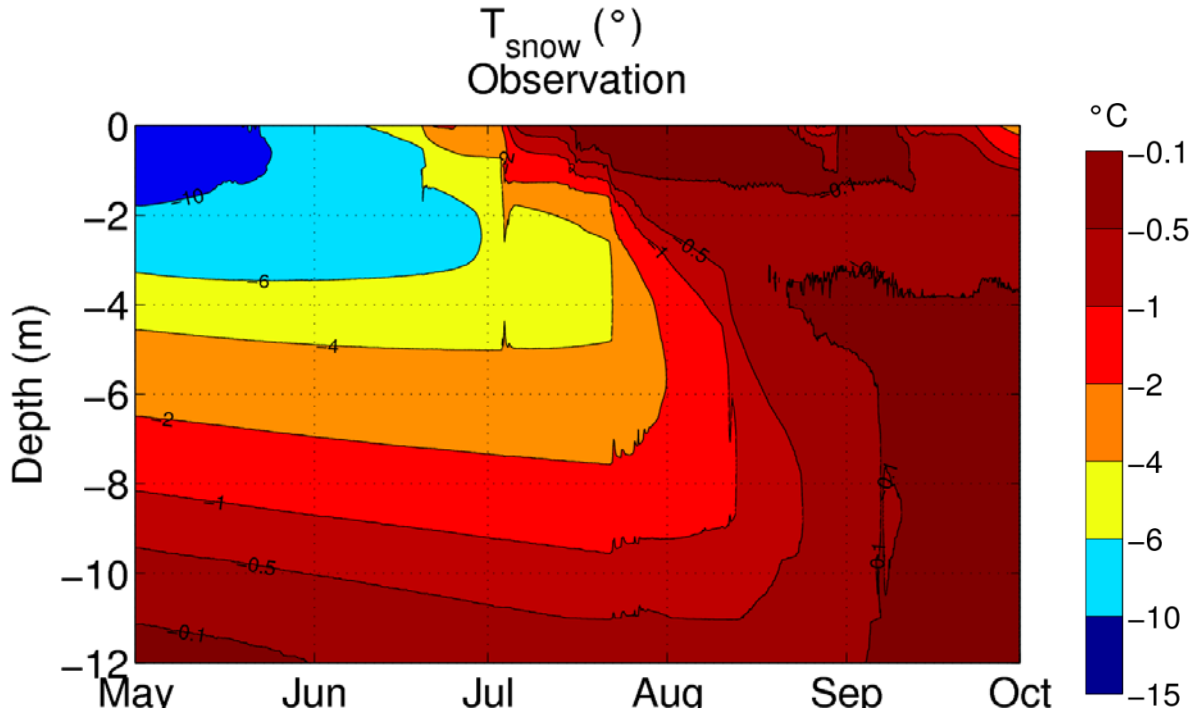

Figure 4. Observed snow temperature evolution at Lomonosovfonna.

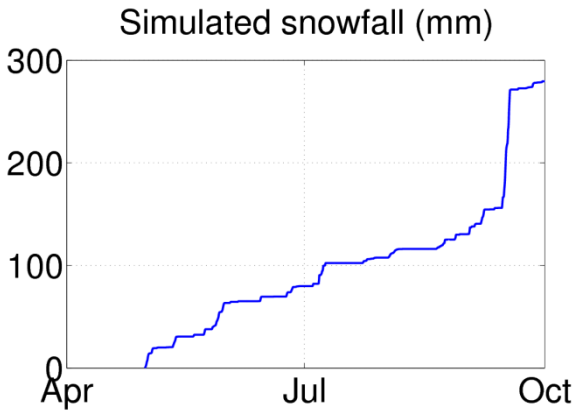

Fig. 5. Simulated accumulated snow fall in mm w.e. since 1 May 2012.

In Fig. 6 the observed density profile from 13 April 2012 is shown. Also shown are the mean densities for the layers represented in Noah-MP with 2 and 5 m w.e. and CLM4 with 1 m w.e. In CLM4 with 2 m w.e. the density in the deepest layer at this date is close to 400 kg m^{-3} as for the observations at this layer depth. The density in the snow layers represented by the snow schemes should thus be about 400 kg m^{-3} for CLM4 and 410–480 kg m^{-3} in Noah-MP. The firn in the model should be around 500 kg m^{-3}. The latter is in agreement with the thermal conductivity expression used for firn if assuming the Sturm et al. (1997) relation.

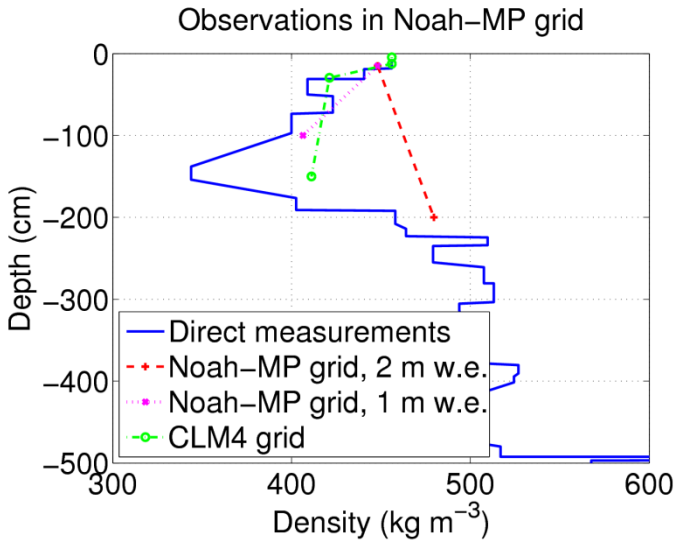

Figure 6. Density profiles from the measurements on Lomonosovfonna on 13 April 2012. Also shown are layer means taken at the depths of the WRF model snow schemes.

Comparison to observations

For the comparison of the simulated snow temperatures we have to bear in mind the different resolutions of the observations and the simulations. The upper level observations are at the best resolved by 0.5 m and then by 1 m. In the Noah-MP simulations the upper two layers are 5 and 20 cm, adding up to 25 cm, and then a bulk layer that can be several meters thick. In CLM4 the 4 upper layers are better resolved, adding up to 41 cm. The lower layer can also here be several meters thick.

In Fig. 7 the temporal evolution of the snow and firn temperature, as simulated by Noah-MP, is shown. The observations and a close-up view of those are shown in the top for comparison. Also shown, in the bottom, are differences to the observations interpolated to the model grid for two of the simulations. Blue thick line indicates boundary between snow and firn in the model. The temperatures represent mean temperature in the layers, which explains why minimums and maximums can be found about a meter above the snow–firn boundary.

With 8 months of spin-up before May, and using the original scheme (*Ref*), similar temperatures are reached in the upper two meters (snow depth is between 4 and 5 m) in the beginning of the investigates period. Later in the period it is evident that the percolation of water is not sufficient. The cold spell in late August is captured but with colder temperatures, probably due to that the near-surface temperature in the observations are actually deeper than when the thermal strings were installed. In Fig. 8 the temporal evolution of the snow temperature, as simulated by CLM4 is shown. In the *Ref* case with 8 months of spin-up the cold wave is warmer than the observations. The percolation of melt water reaches the lower snow layer faster than in Noah-MP and the observations. Already in mid-June the temperature is close to zero throughout the snow pack. It stays warm until mid-September.

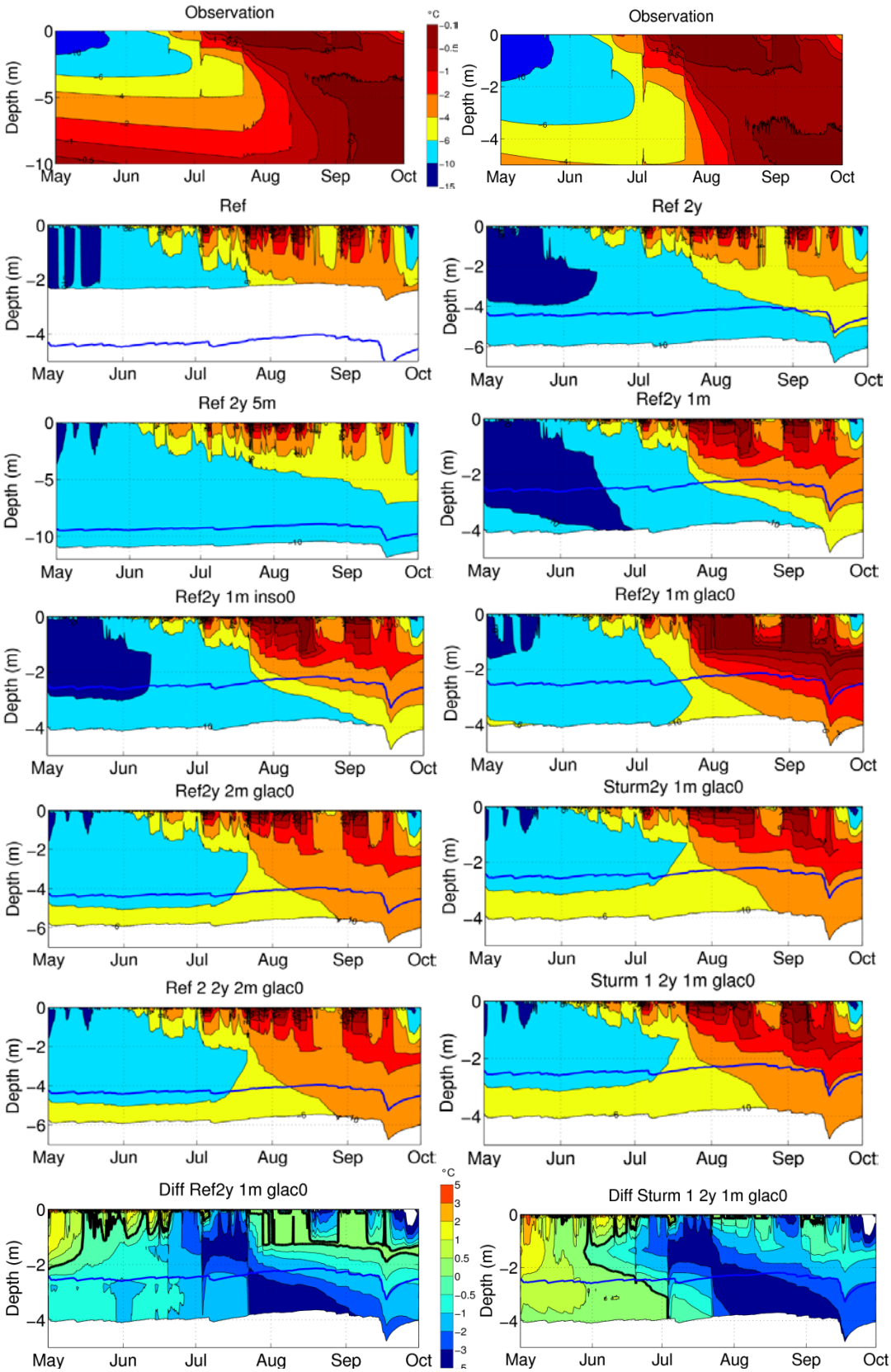

Figure 7. Temporal evolution of snow temperature from the observations at Lomonosovfonna and the Noah-MP scheme. Fields stop at the centre of the lowest layer depth. Blue line show the snow depth in the snow scheme. Shown are also the difference to observations of the best simulations.

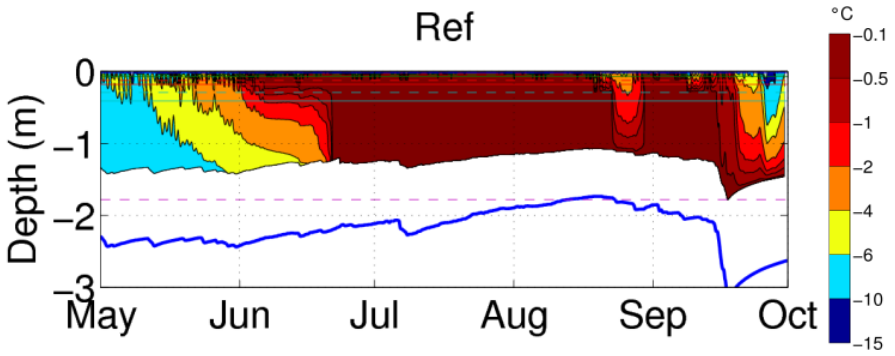

Figure 8. Temporal evolution of snow temperature from the CLM4 scheme. Temperature stops at the centre of the lowest layer depth. Blue line show the snow depth in the snow scheme.

If comparing Noah-MP and CLM4 (Fig. 8) it is evident that the surface snow layers are heated up much earlier in CLM4. With the same temperature forcing this may be related to the short wave radiation and the albedo. Now, the albedo is higher in CLM4 in April and May, but the SNICAR scheme allows penetration of short wave radiation into the upper snow layers and heat absorption in the second to fourth layer (not shown here) from the end of April. This is most probably the explanation of the early heating. Unfortunately this cannot be supported by the observations since the upper thermistors are probably buried with several centimetres of snow, maybe above ten.

The effect of spin-up can be tracked in Fig. 7 with the Noah-MP simulations. With another year of spin-up the cold content becomes larger (colder than the observations) but does not change much the evolution when the melt period starts. Using the longer spin-up and deeper snow (5 m w.e. and around 10 m of snow) included in the calculations (*Ref_2y_5m*) shows that the cold wave is more or less present the whole summer. Either this means that the thermal conductivity is too low, or that there is not enough water to eliminate the cold content. If limiting the snow to 1 m w.e. (*Ref_2y_1m*) increases the temperature of the lowest snow layer and also the firn. Still the snowpack is not heated to melting as in the observation. Further, the timing of the start of melt is not significantly changed.

Initializing the firn layers to 0°C and with 1.5 years of spin-up and 1 m w.e. snow (*Ref2y 1m inso0*) has a rather small effect and only decrease the cold content somewhat in the firn. By initialising also the lower boundary temperature from the annual mean temperature of about –14°C to 0°C (*Ref2y 1m glac0*), however, improves the results significantly. Firn temperature exceeds –4°C in late September and 0°is reached in the lowest snow layer. Thus there is an improvement but still some additional parameter changes are needed. Increasing the snow to 2 m w.e. again (*Ref2y 2m glac0*) reduces the temperature, due to the "inertia" of the thicker deep snow layer. Therefore we focus the physical parameter analysis to the 1 mwe simulations.

The effect of the snow heat conductivity can be tracked by comparing the (*Ref2y 1m glac0*) and (*Sturm2y 1m glac0*) simulations (Fig.7). The lower thermal conductivity in the Sturm

simulation leads to lower cold content but the *Ref* case is a little closer to the observations (see also difference plot in Fig. 7). During the summer the heating is not equally fast as in the Ref case and it is hence colder than the observations. The lowest snow layer only reach –1°C and the firn is also too cold.

By decreasing the water holding capacity (WHC, *Sturm* and *Sturm 2* in Fig. 7) from 3 to 2% would mean that more water percolates down to next layer. All layers except the lowest reach the maximum value a couple of times each summer. However, with this change, the amount of water is not sufficient to significantly change the temperatures when the water refreezes more than in the upper layers. Reducing the WHC to 1% heats the 3rd snow layer but only a few tens of a degree (*Sturm 1* in Fig. 7, including diff plot).

The simulated density generally increases in all layers with time. Surface layers consisting of fresh snow have lower density, which also increases abruptly during melt. For the upper layers the density does not exceed much over 450 kg m^{-3}. For the deepest layer the compaction due to the weight of the above layers is the most important process if the melt is small compared to the mass of snow in this thick layer and may exceed 500 kg m^{-3} in September in some simulations. The compaction will decrease the snow height even if the mass is the same. In April and in the Noah-MP simulations the density is close to 440 kg m^{-3} for the 1 mwe case *Ref2y 1m glac0* and 480 kg m^{-3} for the 2 mwe case (*Ref2y 1m glac0*), not too far from the observations in either case.

Simulated distribution of ablation

In this section the focus is on the sensitivity of the parameters on the summer melt. We define it here as the change in snow w.e. minus the precipitation between 1 May and 1 Aug. The analysis of the Noah-MP simulations is limited to the ones with 0°C initialisation of the firn and glacier. The reference case is shown in Fig. 9a. Note that the first colour scale corresponds to the reference and the other to the difference subplots. The melt is concentrated to the inner part of Isfjorden and around Barentsburg to the west and south of Isfjorden inlet, and to other low elevation areas.

The effect of deeper snow (2 m compared to 1 m w.e.) is shown in Fig. 9b. A somewhat lower melt covers most of the archipelago with concentrations especially at the southern tip and the north-western part of Spitsbergen, and at the coast of Nordaustlandet.

The effect of the Sturm heat conductivity is seen in Fig. 9c. The effect is mainly that the coasts have less melt with Sturm, except around Isfjorden.

The water holding capacity (WHC) effect is seen in Fig. 9d and 9e for both Yen and Sturm thermal conductivity. As for the temperature the effect is minimal. Even when reducing the WHC to 1% does not change this (not shown).

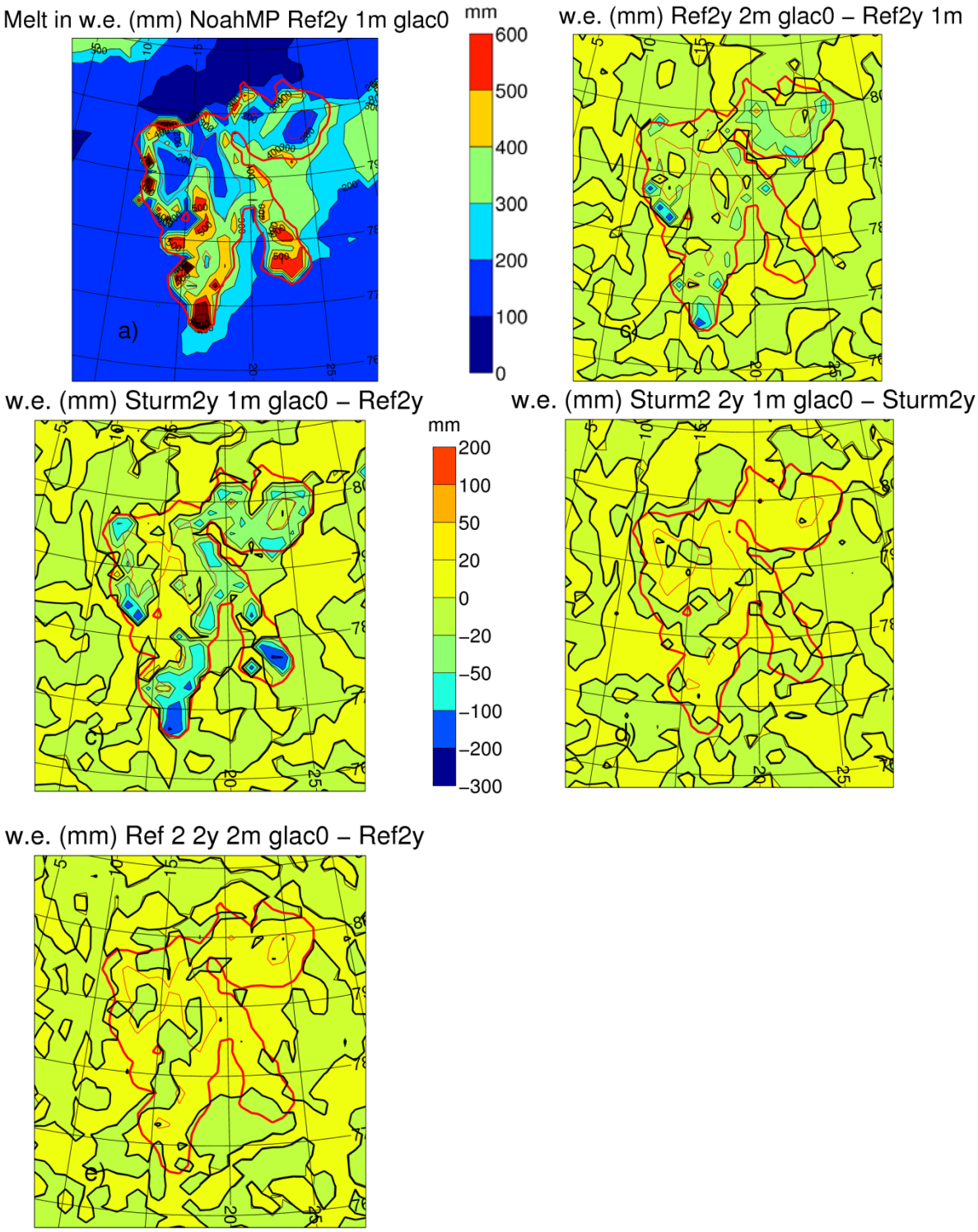

Figure 9. Summer melt in 2012 in mm w.e. from the Noah-MP scheme. Red thin lines show the 500 m elevation of the terrain.

DISCUSSION AND CONCLUSIONS

This study was initiated to find proper values of the snow thermal conductivity and water holding capacity. The snow temperature from the WRF simulations was compared to measurements at Lomonosovfonna. The surface scheme CLM4 was first in focus because it has a very sophisticated albedo scheme and more snow layers. Noah-MP was run as a reference. While the simulations and analyses were performed it was noticed that the CLM4 needed much (five times) more computer resources compared to Noah-MP. After a couple of simulations with CLM4 the focus was instead turned towards Noah-MP. For climate simulations on the order of 20 years with 5.5 km horizontal resolution (in this study 16.5 km) it is not practicable to use CLM4 but for short-period studies it can be interesting. Further the initialization and spin-up time could be of importance as well and the spin-up period was prolonged one year to capture a better cold wave and the higher temperatures left from previous year's summer melt. Also the soil layers, defined as firn over glaciers, were included in the temperature analysis.

The analysis of the simulations pointed out the importance of correct initialisation, even if the spin-up time was more than one year, covering a hydrological cycle. At least for Lomonosovfonna there was a need of setting all layers to 0°C, even the glacier boundary condition to the firn. By doing so, the temperature was improved significantly in relation to the observations.

The effect of thickness was investigated as well. Just the lowest layer was changed because we wanted the resolution in the top layers to be as good as possible to capture the thermal and hydrological forcing from the surface. The thickness was both reduced and increased. On the first hand a reduction can improve the resolution and possibly the calculations. On the other hand, a deep layer included more of the deeper snow and firn and may thus better take care of the influence from the deep temperatures. The analysis showed that a thinner layer (1 m w.e.) better represents the snow pack temperature evolution at Lomonosovfonna, but this also requires that the glacier temperature is set to 0°C. This, however, limits the comparison down to about 4 m, including firn. In the observations the cold wave penetrates deeper than 10 m. However, to be able to classify the soil as firn, the seasonal snow should be represented by the snow model. Therefore it should cover at least more than the maximum annual precipitation probably more than 1.5 m w.e. (cf. Claremar et al. 2013b) in southern Spitsbergen but the depth should still not cover more than 2 m. At Lomonosovfonna the annual precipitation is close to 1 m according to the simulations in 16.5 km resolution and 1.4 m in 5.5 km resolution.

The most important parameter seems to be the snow thermal conductivity. Changing the water holding capacity does neither significantly change the water leaving the modelled snow pack or the temperature. This depends probably on the low amount liquid water available to refreeze compared to the mass of the snow in the deep thick layer. This might change by reducing WHC even more and by implement it in the firn layers as well. Throughout the period the Yen (1965) expression performs somewhat better and the bias to observations are of different sign in the spring period for the two expressions. But the influence from possible

errors in atmospheric temperature and the surface energy balance may prevent us from drawing any robust conclusions about which one is the better. Unfortunately there are no albedo or energy balance data locally at Lomonosovfonna for this year but for 2013, which will be investigated in the future work. Thermal conductivity is not solely dependent on the density but is basically a function of the inter-connection areas between the snow grains (e.g. Domine et al. 2011). This is partly dependent on the density but freeze-thaw cycles increases this area, even if the density change is small. Therefore one may expect that the relevant expression may change through time. The snow thermal conductivity can also be expressed as a function of density together with shear strength. Shear strength can be measured in the field by rotating the snow with a shear vane and finding the maximum torque. It can also be modelled, but this is outside the frame of this investigation. Not accounted for here is the process of wind packing of the snow (which will be buried after new snow fall). This effectively increases the thermal conductivity but is rather much related to the density alone (Sturm et al. 1997). The thermal conductivity of the firn can be more deeply investigated.

It will not be possible to model ice-layers other than in the top snow layer, or layers, in the present versions of Noah-MP and CLM4. The thickness is too large to increase the density by refrozen liquid water. None of the snow schemes made it possible to increase the number of snow layers. What can be done is to change the layer thicknesses.

Related to bullet 2 in the introduction are the different snow regimes on the glaciers. If possible, glacier ice should be taken into account below the ELA. There are algorithms available for quantifying the development of superimposed ice. To find bare ice (and no firn) may require height information in the snow scheme subroutine or a new glacier bare ice mask. In the Noah-MP snow schemes and with ERA-Interim as input glaciers are interpreted as tens of meters of snow and is in the initial step transformed to snow only in the snow model domain (1–5 m w.e. in this study) and firn in the soil domain (2 m thickness).

The time frame limited the conclusions regarding the proper snow parameters. However, the work continues in the spring and will be presented in a submitted manuscript. Observations for more years and from other sites on Svalbard (e.g. Kongsvegen, Kronebreen and Holtedahlsfonna) will be used and more parameter set-ups will be investigated. Available energy observations will also help tuning the summer heat balance to provide better surface forcing of the snowpack. Further, the equilibrium level altitude (ELA) on the Svalbard archipelago will be estimated for the simulated year or years and compared to observed values. Albedo and snow products from MODIS satellite images may also be utilized to find snow lines.

To conclude:

- CLM4 is not suitable for high-resolution climate simulations. But for limited areas and periods it should be used as far as possible. Otherwise the Noah-MP scheme is useful, given the correct initialisations and snow parameters.

- In CLM4 the surface snow is heated by penetrating short wave radiation that is absorbed by the snow. This is probably why the summer snow temperature is much higher in CLM4.
- The snow thermal evolution is very dependent on the thermal conductivity. The actual thermal conduction relation seems to be in between the investigated expressions by Yen (1965) and Sturm et al. (1997).
- Liquid water does not penetrate sufficiently deep in Noah-MP. The latter may be related to too week heating at the surface, i.e. too high albedo and/or weak short wave penetration.
- Snow scheme should cover 1–2 mwe and the soil/firn temperatures can be analysed together with the snow layers, which represents the seasonal snow.
- If possible, glacier ice without firn, should be taken into account below the ELA. This may not be easily solved in the present snow scheme subroutine.
- A coming manuscript will try to find the better WHC and thermal conductivity of the snow/firn since observed surface energy balance will be available.

Acknowledgements

Sergey Marchenko and Veijo Pohjola at Uppsala University and Carl Egede Bøggild at DTU are thanked for input and discussions. Thanks to Kjetil Schanke Aas I could get use of the OSTIA data provided by MYOCEAN and the glacial mask from NPI. Carleen Reijmer at University of Utrecht provided the AWS data from Nordenskiöldbreen. Simulations were performed at UPPMAX, Uppsala University. The work was funded by the Nordic council of ministers (SVALI, www.ncoe-svali.org).

References

Anderson, E.A. (1976). A point energy mass balance model of a snow cover. NOAA Tech. Rep. NWS 19, 150 pp., Off. of Hydrol., Natl. Weather Serv., Silver Springs, Md.

Claremar, B., Obleitner, F., Reijmer, C., Pohjola, V., Waxegård, A. et al. (2012). Applying a Mesoscale Atmospheric Model to Svalbard Glaciers. Advances in Meteorology. 321649

Claremar, B 2013a. Relation between meso-scale climate and glacier/snow mass balance on Svalbard. SVALI report D2.3-11.

Claremar, B 2013b. Water retention parameterization in the WRF model — A sensitivity test. SVALI report D3.1-1.

Dee, D. P., Uppala, S. M., Simmons, A. J., Berrisford, P., Poli, P., et al. (2011). The ERA-Interim reanalysis: configuration and performance of the data assimilation system. Q.J.R. Meteorol. Soc., 137: 553–597. doi: 10.1002/qj.828

Domine et al. 2011. Linking the effective thermal conductivity of snow to its shear strength and density.

Donlon et al. 2012, The Operational Sea Surface Temperature and Sea Ice Analysis (OSTIA) system. Remote Sens. Environ., 116, 140–158.

Dunse, T. et al. 2009. Recent fluctuations in the extent of the firn area of Austfonna, Svalbard. Ann. Glac.

Jordan 1991. A one-dimensional temperature model for a snow cover. CRREL SP 91-16.

Lawrence et al. 2011. Parameterization Improvements and Functional and Structural Advances in Version 4 of the Community Land Model. J. Adv. Model. Earth Sys., 3, DOI: 10.1029/2011MS00004.

Marchenko S. 2012. Thermal regime, stratigraphy and density of the active layer at Nordenskiöldbreen (Spitsbergen) as principle controls on meltwater refreezing rates. Scientific report, Ymer-80 Foundation.

Marchenko S. 2013. Controls on and rates of water flow, storage and refreezing in snow/firn/icepack at Lomonosovfonna, Spitsbergen. Scientific report, Ymer-80 Foundation.

H. Morrison, J. A. Curry, and V. I. Khvorostyanov (2005), A new double-moment microphysics parameterization for application in cloud and climate models. Part I: Description. J. Atm. Sci., vol. 62, no. 6, 1665–1677.

Nakanishi, M. and Niino H. (2006), An Improved Mellor–Yamada Level-3 Model: Its Numerical Stability and Application to a Regional Prediction of Advection Fog, Boundary-Layer Meteorol., vol. 119, no. 2, pp. 397–407.

Niu, G.-Y., Yang Z.-L., Mitchell K.E., Chen F., Ek, M.B., et al 2011. The community Noah land surface model with multiparameterization options (Noah-MP): 1. Model description and evaluation with local-scale measurements. J. Geophys. Res., 116, D12109, doi: 10.1029/2010JD015139.

Nuth et al. 2013. Decadal changes from a multi-temporal glacier inventory of Svalbard. The Cryosphere Discuss., 7, 1603–1621.

Schneider, T. and Jansson, P 2004. Internal accumulation in firn and its significance for the mass balance of Storglaciären, Sweden. J. Glaciol., 50, 25–34.

Shumskii P. A. 1955 Osnovi strukturnogo ledovedeniya (Principles of structural glaciology), Akademia Nauk, Moscow (in Russian).

Shumskii P. A. 1964 Principles of structural glaciology, translation by David Kraus, Dover Publications, Inc., New York

Skamarock, W. C. et al. 2008, "A description of the Advanced Research WRF version 3". NCAR Technical note TN-475 + STR. Boulder, Colorado, USA, 113 pp., 2008.

Sturm, M., Holmgren, J., König, M., and Morris, K. 1997. The thermal conductivity of seasonal snow, J. Glaciol., 43, 26–41.

Sun, S., Jin, J.M., and Xue, Y 1999. A simple snow-atmosphere-soil transfer model. J. Geophys. Res., 104, 19,587–19,597, doi: 10.1029/1999JD900305.

Yang Z.-L. and G.-Y. Niu 2003. The versatile Integrator of surface and atmospheric processes (VISA) part 1: Model description. Global Planet. Change, 38, 175–189, doi: 10.1016/S0921-8181(03)00028-6.

Yang, Z.-L., R. E. Dickinson, A. Robock, and K. Y. Vinnikov, 1997. Validation of the snow sub-model of the Biosphere-Atmosphere Transfer Scheme with Russian snow cover and meteorological observational data, J. Clim., 10, 353–373, doi:10.1175/1520-0442(1997)010<0353:VOTSSO>2.0.CO;2.

Yen YC. 1965. Heat transfer characteristics of naturally compacted snow. US Army Cold Regions Research and Engineering Laboratory, Research Report 166, Hanover, NH, 9 pp.

Yen, Y.-C., (1981), Review of thermal properties of snow, ice and sea ice, Cold Regions Research and Engineering Laboratory (CRREL) Report 81-10, U.S. Army Cold Reg. Res. and Eng. Lab., Hanover, NH.

Zagorodnov, V.S. 1985. Ldoobrazovaniye i glubinnoye stroyeniye lednikov [Ice formation and inner structure of glaciers]. In Kotlyakov, V.M., ed. Glyatsiologiya Shpitsbergena [Glaciology of Spitsbergen]. Moscow, Nauka, 119–147